J Mater Sci: Mater Med (2008) 19:1225–1233
DOI 10.1007/s10856-007-3163-x

The behaviour of selected yttrium containing bioactive glass microspheres in simulated body environments

D. Cacaina · H. Ylänen · S. Simon · M. Hupa

Received: 19 May 2006 / Accepted: 28 August 2006 / Published online: 15 August 2007

Abstract The study aims at the manufacture and investigation of biodegradable glass microspheres incorporated with yttrium potentially useful for radionuclide therapy of cancer. The glass microspheres in the SiO_2–Na_2O–P_2O_5–CaO–K_2O–MgO system containing yttrium were prepared by conventional melting and flame spheroidization. The behaviour of the yttrium silicate glass microspheres was investigated under in vitro conditions using simulated body fluid (SBF) and Tris buffer solution (TBS), for different periods of time, according to half-life time of the Y-90. The local structure of the glasses and the effect of yttrium on the biodegradability process were evaluated by Fourier Transform Infrared (FT-IR) spectroscopy and Back Scattered Electron Imaging of Scanning Electron Microscopy (BEI-SEM) equipped with Energy Dispersive X-ray (EDX) analysis. UV–VIS spectrometry and Inductively Coupled Plasma Mass Spectrometry (ICP-MS) was used for analyzing the release behaviour of silica and yttrium in the two used solutions. The results indicate that the addition of yttrium to a bioactive glass increases its structural stability which therefore, induced a different behaviour of the glasses in simulated body environments.

D. Cacaina · S. Simon
Faculty of Physics, Babes-Bolyai University,
M. Kogalniceanu 1, Cluj-Napoca 400084, Romania

D. Cacaina (✉) · H. Ylänen
Turku Biomaterials Centre, University of Turku,
Itäinen Pitkäkatu 4 B (PharmaCity), Turku 20500, Finland
e-mail: dana.cacaina@utu.fi

M. Hupa
Process Chemistry Centre, Åbo Akademi University,
Biskopsgatan 8, Turku 20500, Finland

Introduction

Internal radionuclide therapy using microspheres incorporating beta emitters represents an alternative for cancer treatment, especially for cancers where the response to chemotherapy and external radiotherapy is poor like liver cancer [1–3]. Non-biodegradable and biodegradable microspheres containing short-range beta radioisotopes have been investigated for possible use in therapeutic applications [3–5]. Inert radioactive glass microspheres currently in use for the treatment of liver metastases remain as impurity in the target area after the radioactivity decays [1, 2]. Thus, the dissolution and elimination of the glasses from the body would be desirable.

In the present study yttrium was added to the composition of a bioactive glass in order to develop a biodegradable glass system able to carry the radiation inside the cancer site and provide a high and localized dose of beta radiation. Yttrium is a beta-emitter with suitable nuclear properties for radiotherapeutic purposes [1].

Since discovered by Hench in 1969 [6], bioactive glasses have been intensively investigated due to their successful use in various clinical applications. The main characteristic of bioactive glasses is their chemical and biological in vivo activity. It is known that a partial dissolution of the bioactive glass occurs when they are exposed to human plasma or an analogous solution [6–9].

The mechanism of the degradation of bioactive glass was proposed by Hench et al. [6] and involves three main processes: ion exchange, dissolution and precipitation. Ion exchange occurs at the bioactive glass surface, in which cations such as Na^+ and Ca^{2+} from the glass are exchange to H^+ and H_3O^+ from the surrounding solution. During the dissolution, the glass silica network is partially broken through the action of hydroxyl (OH^-) ions. Breakdown of

the network occurs locally and releases silica into solution in the form of silicic acid ($Si(OH)_4$). The rate of dissolution depends on the glass composition. The hydrated silica (SiOH) formed on the glass surface by these reactions undergoes rearrangement by polycondensation of neighbouring silanols, resulting in a silica-rich layer. Precipitation of the calcium and phosphate ions released from the glass together with those from solution form a calcium phosphate-rich layer on the surface [6, 8, 9].

The aim of the present study was to investigate the behaviour of yttrium containing bioactive glasses in simulated body environments. The investigated glass samples were prepared by melt annealing method. The degradation of the glass samples and the local structural changes occurred in the glass network during the immersion in the two used solutions was analyzed by BEI-SEM/EDX analysis and Infrared spectroscopy.

Experimental

The glass samples were prepared by mixing the analytical grade Na_2CO_3, K_2CO_3, MgO, $CaCO_3$, $CaHPO_4(2H_2O)$, Y_2O_3 and commercial Belgian quartz sand and melting the batches in a Pt-crucible at 1360 °C and 1450 °C for the high yttrium content glass, for 3 h. The compositions of the yttrium containing glasses and the reference bioactive glass are given in Table 1. The glasses were cast, annealed, crushed and remelted to improve homogeneity.

The microspheres were obtained by flame spheroidization, process in which the glass granules with a diameter of 90–150 μm for the yttrium bioactive glasses and 125–250 μm for the bioactive glass were passed into a gas/oxygen flame, where each molten particle becomes spherical due to the surface tension [10].

The stability tests were carried out by immersing glass microspheres in a simulated body fluid (SBF) and 0.05 M Tris buffer solution (TBS) [11] with a pH at 7.4 and kept at 37 °C, under continuous agitation, for up to 27 days. Different amount of microspheres were immersed in 25 mL solution in order to keep a ratio between glass surface area (SA) and solution volume (V) close to 0.4 cm^{-1} [12]. At each immersion time point, 5 mL of the solution was taken off and the same amount of fresh solution was added. The yttrium and silica release behaviour in the solution was analyzed using ICP-MS and UV–VIS spectrophotometer.

At the end of the immersion period, the samples were taken out from the fluid, rinsed with ultra pure water and ethanol, and dried. Some of the immersed microspheres were embedded in acrylic resin for BEI-SEM analysis. After hardening the samples were sectioned and polished. The polished surface was coated with a thin layer of carbon. By scanning electron microscopy the reaction layers formed on the glass microspheres during immersion in solutions were analyzed. EDX analysis was used for the elemental identification of the reaction layers.

Information on the active Si–O groups present in the glass network of the as-prepared and reacted samples was obtained by FT-IR spectroscopy. All spectra were obtained between 4000–400 cm^{-1} wave number, using powder/KBr pellets.

Results and discussion

The BEI-SEM images of the bioactive and yttrium containing bioactive glass microspheres immersed in SBF are shown in Figs. 1 and 2. According to EDX analysis, in cross section of a bioactive microsphere (Fig. 1) three different zones were identified: the original glass (spot 1), a silica-rich layer (spot 2) and on the top of silica-rich layer a calcium phosphate layer (spot 3).

The calculated molar ratio between Ca and P, from the EDX analysis, of the calcium phosphate layer was 1.6, thus close to the Ca/P ratio in the hydroxyapatite. Almost the same composition is evidenced for the precipitate particles (spot 4). The results are in good agreement with those reported in the literature [8, 9].

While on the bioactive glass two reaction layers of different composition were identified, for the glasses containing yttrium only one reaction layer was detected on the glass surface after immersion in SBF. This reaction layer is rich in calcium, phosphorus and yttrium, confirmed by EDX analysis (Fig. 2 spot 2). For this layer, the molar ratio between Ca and P, calculated from EDX analysis, was approximately half of the Ca/P ratio in the hydroxyapatite. When exposed to SBF, the yttrium containing glass surface starts to dissolve. By time, the solubility product of calcium phosphate is exceeded resulting in precipitation of yttrium

Table 1 Composition of the investigated glasses (% wt)

Glass	SiO_2	Na_2O	P_2O_5	CaO	K_2O	MgO	Y_2O_3
HB1	53	6	4	20	12	5	0
HY1.1	46.09	5.22	3.48	17.39	10.43	4.35	13.04
LYS	53	6	2	10	12	2	15

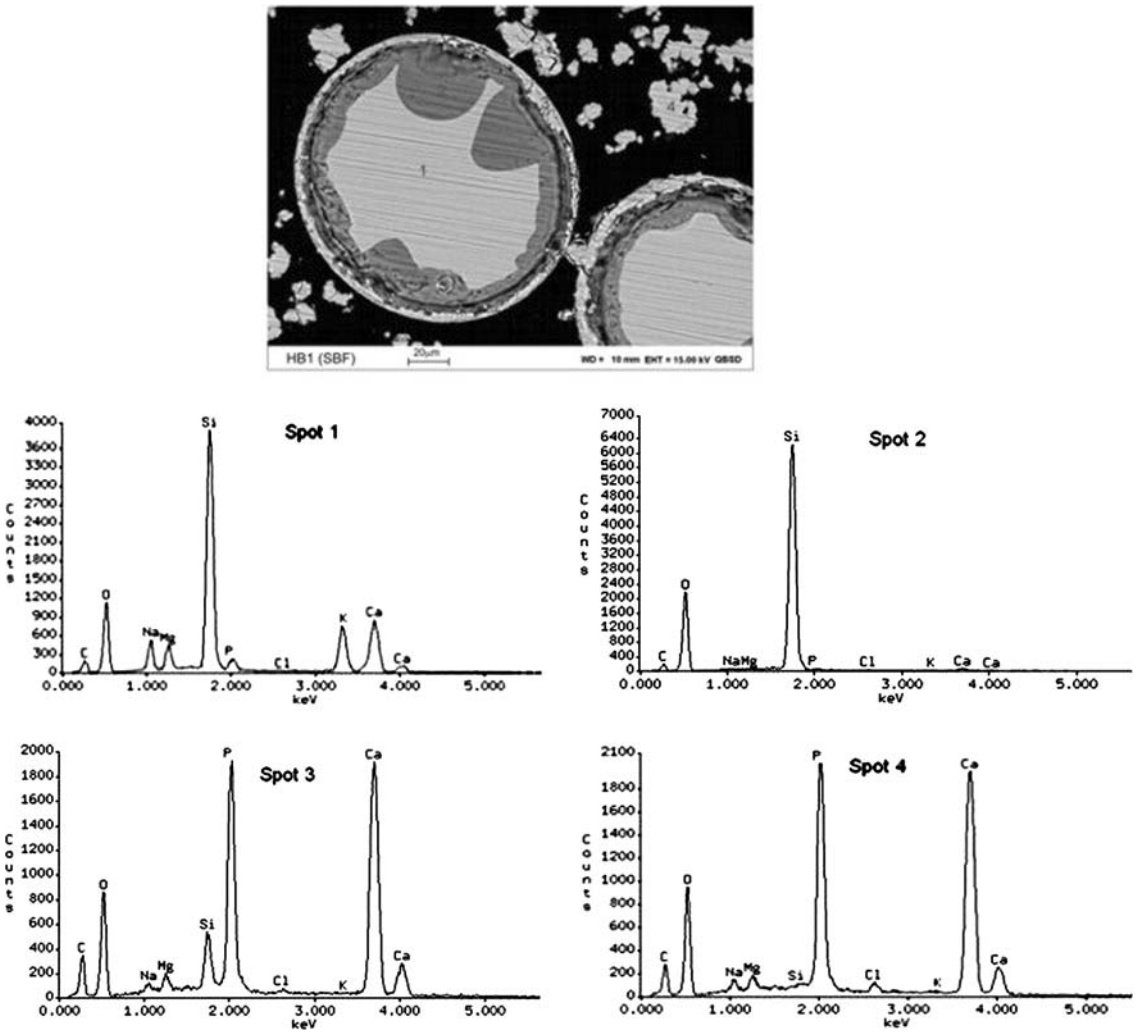

Fig. 1 BEI-SEM image and EDXA spectra for HB1 glass microspheres after immersion in SBF. According to EDXA: spot 1—glass, spot 2—Si-rich layer, spot 3—CaP layer, spot 4—CaP compound

calcium phosphate on the surface of the microspheres. The formation of the yttrium-rich layer on the surface of the microspheres indicates the degradation of the glasses in solution.

The BEI-SEM analysis of the immersed microspheres in the TBS show also a reaction layer formation on the surface of the microspheres due to the reactions occurred at the microsphere—solution interface. Figure 3 show the cross section image of the reacted bioactive microspheres. According to the EDX analysis, the exchange reactions at the microspheres surface lead to the formation of a silica-rich layer. No detectable calcium phosphate layer was found on the microspheres surface in TBS. The precipitation of calcium and phosphorus released from the glass into the solution does not occur due to the small amount of phosphorus in the glass composition and the absence of these ions in the immersion solution.

For yttrium glasses, the rate of ion exchange is lower than that for bioactive glass. Therefore, there is no reaction layer after immersion in TBS, clearly detectable by BEI-SEM (Fig. 4). The linescan EDX analysis on the cross section of the microspheres after immersion TBS indicates the presence of a thin region rich in silica on their surface, formed due to the ion exchange reaction occurred in the solution. Moreover, the small amount of silica and yttrium released into the solution, determined by ICP-MS and UV–VIS spectrometry, indicates that chemical reactions occurred at the glass—solution interface.

The UV–VIS spectrometry (Figs. 5–7) measurements show the concentration of silica released in the two used solutions. The release of silica indicates the dissolution of the glass during immersion in the solutions. For the all investigated glasses, the silica concentration in the solutions increased with the immersion time. A different trend

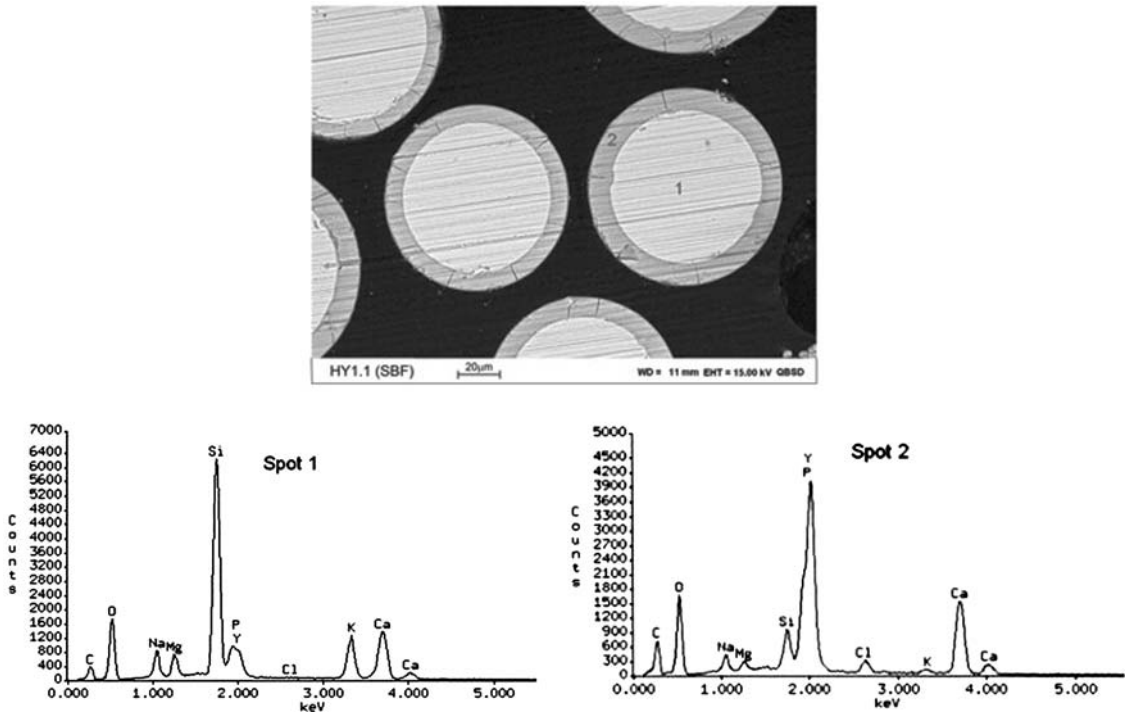

Fig. 2 BEI-SEM image and EDXA spectra for HY1.1 glass microspheres after immersion in SBF. According to EDXA: spot 1—glass, spot 2—CaP layer rich in yttrium

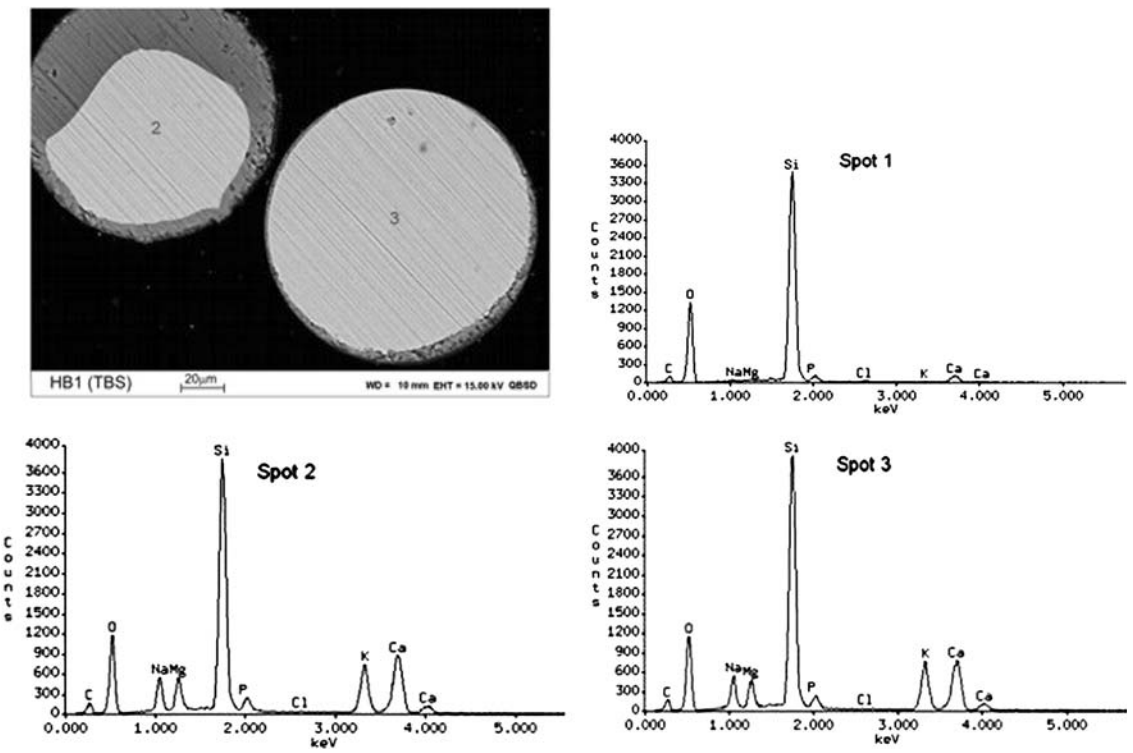

Fig. 3 BEI-SEM image and EDXA spectra for HB1 glass microspheres after immersion in TBS. According to EDXA: spot 1—Si-rich layer, spots 2 and 3—glass

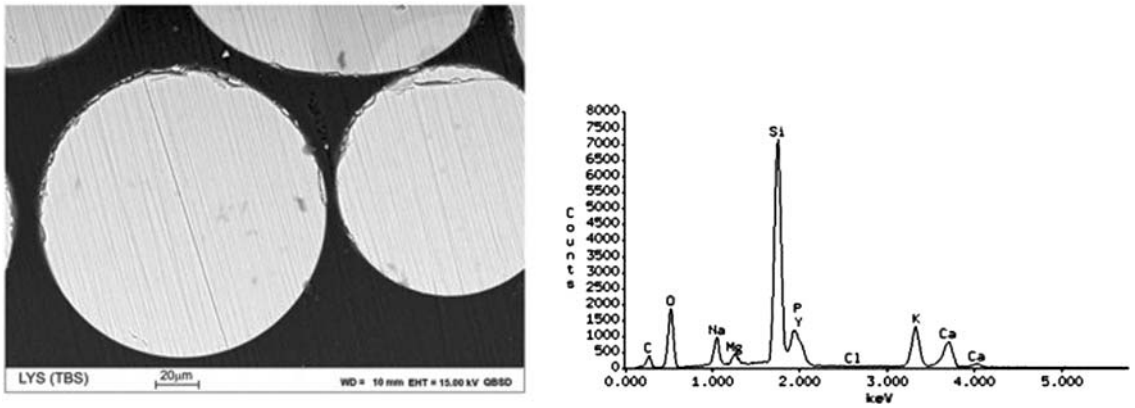

Fig. 4 BEI-SEM image and EDXA spectra for LYS glass microspheres after immersion in TBS

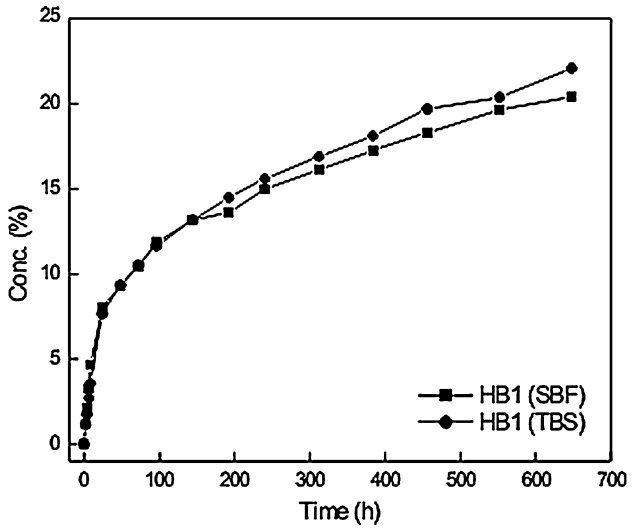

Fig. 5 The concentration of silica released from the HB1 microspheres into SBF and TBS

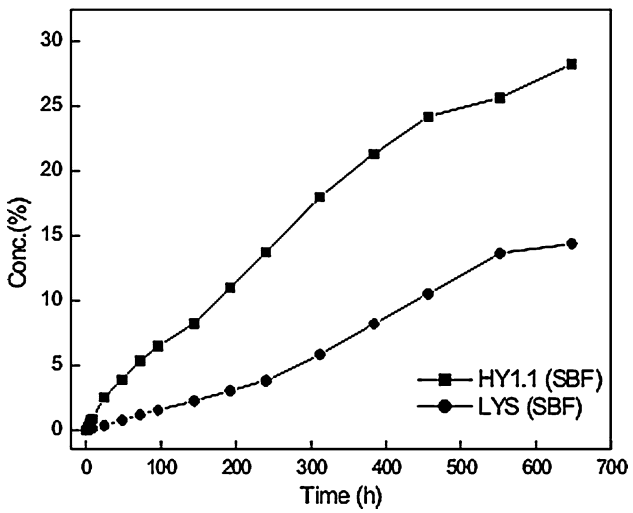

Fig. 6 The concentration of silica released from the HY1.1 and LYS microspheres into SBF

of the silica release behaviour for the reference bioactive glass and yttrium bioactive glasses can be seen.

For the bioactive glass the same silica release behaviour could be observed in the two used solutions (Fig. 5), which is in good agreement with the literature [13]. Silica is released fast in the first immersion stage, up to 72 h and then the release is almost linearly. When exposed to body fluids a dealkalisation of the glass surface occurred, due to the exchange of ions from the glass with the H_3O^+ and H^+ from the solution. Network dissolution occurs concurrently by breaking of –Si–O–Si–O–Si– bonds through the action of OH^- ions [6, 8, 9]. The dissolution reaction results in release of silica into solution. These reactions lead to the formation of silanol groups on the surface of the microspheres. As a consequence of the condensation and polymerization of the silanol groups, a layer rich in silica is formed on the surface of the micrcospheres.

For the yttrium bioactive glasses the silica release behaviour is different than that for the reference bioactive glass in both used solutions (Figs. 6 and 7). As can be observed, the silica is almost linearly released into the SBF solution, and during the first immersion stage the release is lower than for the reference bioactive glass (Fig. 6). The different release behaviour could be explained by the presence of yttrium in the glass structure and in the calcium phosphate layer developed on the glass surface during the immersion in SBF. The fast deposition of calcium and phosphorus on the surface of the yttrium bioactive microspheres leads to the formation of a thicker calcium phosphate layer rich in yttrium than the calcium phosphate layer formed on the reference bioactive microspheres [14]. This calcium phosphate layer rich in yttrium formed in the early immersion stage could retard the leaching reactions and consequently the growth of silica-rich layer. However, the release of silica indicates that the dissolution of the glass occurs in the SBF solution.

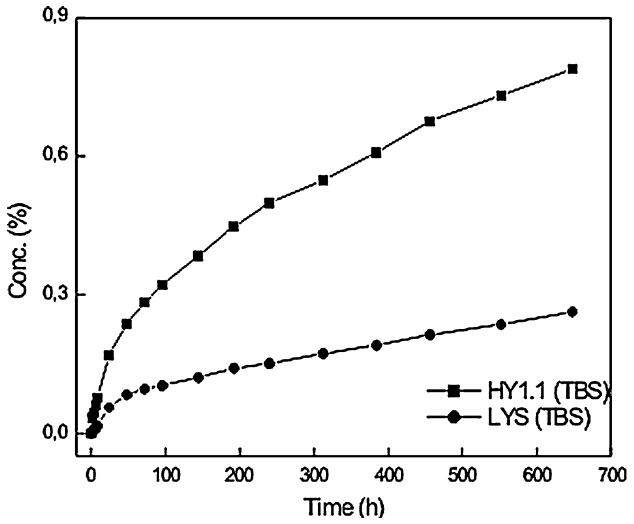

Fig. 7 The concentration of silica released from the HY1.1 and LYS microspheres into TBS

The trend of silica release in TBS for yttrium bioactive glasses is shown in Fig. 7. As can be observed, for the yttrium bioactive glasses the concentration of silica released in TBS is less than in SBF solution while for the bioactive glass the concentration of silica released in the two used solutions is almost the same. In general, the corrosion of the glass in the solution can be described by ion exchange and network dissolution reactions.

The ion exchange and silica dissolution reactions are controlled by the local pH at the interface sample—solution. According to the literature [13], below pH = 9 the ion exchange is constant and the silica dissolution is also constant, but small. The silica dissolution increases rapidly above this pH and for pH > 9.5 it becomes dominant.

In case of using a SBF solution, the ions released from the yttrium bioactive glasses into the solution together with the calcium and phosphate ions deposited from the solution onto the glass surface induced a local increase of the pH. Therefore, the silica dissolution reaction is dominant, which leads to an increase in the silica concentration in the solution.

For TBS, which does not contain the all ions of SBF solution, the concentration of ions released from the glass sample could not increase the local pH to a value corresponding to high silica dissolution. Hence, in this case the ion exchange reaction is dominant and the concentration of silica released in the solution is lower than that released in the SBF.

The difference in silica release behaviour for the bioactive and yttrium bioactive glasses could be explained by the increase of the structural stability of the network due to the addition of yttrium to the bioactive composition.

The concentration of silica released in both solutions from the LYS sample is lower than that for the HY1.1 sample. This suggests a higher structural stability of the silica network in LYS sample due to the partial substitution of calcium, magnesium and phosphorus oxides by yttrium oxide. This may be explained by the field strength of the Y^{3+} ion, which is higher than the field strength of the calcium and magnesium ions [14, 15].

Figure 8 shows the release behaviour of yttrium in the SBF solution. As can be observed, the release of yttrium in SBF is fast during the first immersion stage and then almost constant, while in TBS solution yttrium is linearly released (Fig. 9).

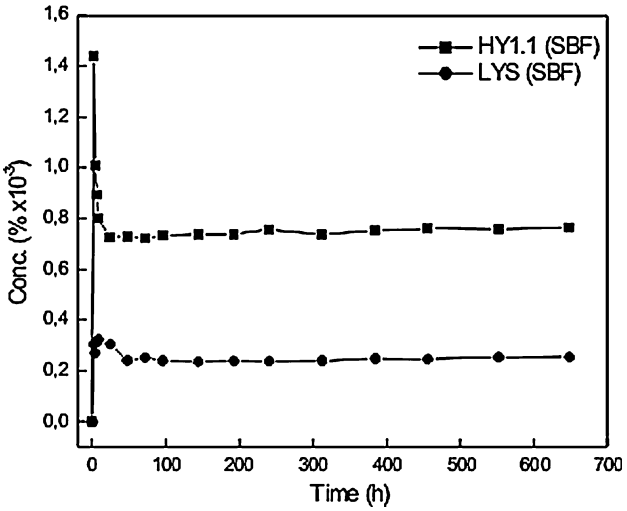

Fig. 8 The concentration of yttrium released from the HY1.1 and LYS microspheres into SBF

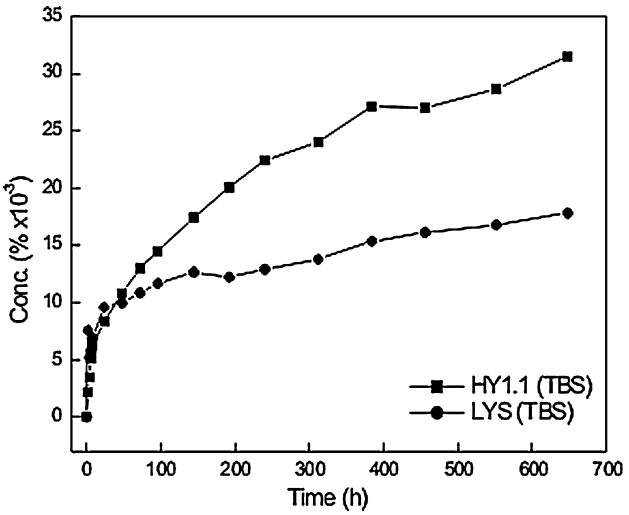

Fig. 9 The concentration of yttrium released from the HY1.1 and LYS microspheres into TBS

During the first hours of immersion, the release of yttrium in SBF is high and then decreased up to 48 h. From this stage on, the concentration of yttrium in the solution slightly varied. The decrease of the concentration of yttrium in SBF is caused by the higher rate of consumption yttrium through the formation of a calcium phosphate layer rich in yttrium on the glass surface than that of releasing of yttrium into the solution. The presence of yttrium in the calcium phosphate layer formed on the surface of the yttrium bioactive glasses is clearly indicated by EDX analysis.

The absorption of Y^{3+} ions to the calcium phosphate rich surface layer leads to the formation of yttrium containing compounds. Moreover, the concentration of yttrium released in TBS is higher than in SBF (Fig. 9). The high concentration of yttrium in TBS could be explained by the absence of yttrium containing calcium phosphate layer on the glass surface. Yttrium was found in large amount in the solution, which means that in TBS no calcium phosphate layer was developed on the microspheres surface to block the yttrium release or to consume yttrium ions.

The concentration of yttrium released from the LYS sample into both solutions is lower than the concentration of yttrium released from the HY1.1 sample. The lower release of yttrium ions from the LYS sample into the used solutions indicates that yttrium ions are better stabilized in this sample network and in the layer formed on its surface. The structural stability of the glass network and of the yttrium ions in the glass network is changed by the different way of adding yttrium to the bioactive glass composition.

The FT-IR spectra of the glass samples show the presence of the typical absorption bands for bioactive glasses (Figs. 10–12).

The structure of silicate glasses can be described in terms of four individual Q^n sites, where n is the number of bridging oxygens in a SiO_4 group [16]. The main bands presented in the as-prepared glass spectra are assigned to the vibration of the Si–O–Si groups.

According to the literature [17–23] the band located in the range of 1000–1100 cm^{-1} is attributed to the Si–O–Si asymmetric stretching vibration mode. The band located in the range 934–950 cm^{-1} is attributed to Si–O with two non-bridging oxygens (Si–O–2NBO) per SiO_4 tetrahedron stretching vibration (Q^2 group). The band is broader due to the high amount of the modifier oxides introduced in the silica network. The addition of high amount of network modifier oxides to a vitreous silica leads to broadening and shifting of the corresponding bands towards lower wave numbers. This is due to the build of SiO_4 tetrahedral units bearing a higher number of non-bridging oxygens than in the vitreous silica. The spectra exhibit also a band located in the range 755–764 cm^{-1} assigned to Si–O–Si symmetric

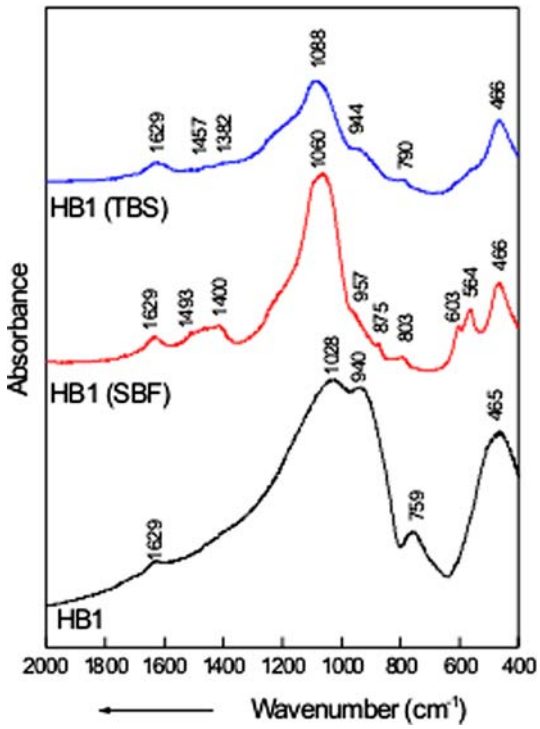

Fig. 10 FT-IR spectra of HB1 sample before and after immersion in SBF and TBS

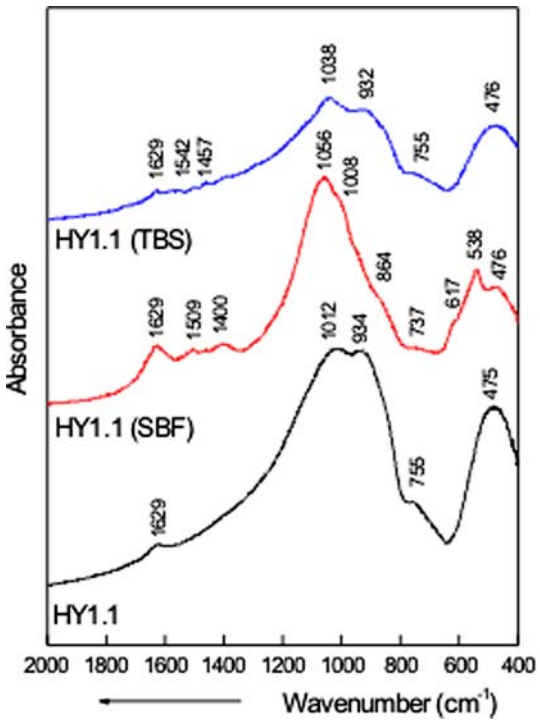

Fig. 11 FT-IR spectra of HY1.1 sample before and after immersion in SBF and TBS

stretching vibration of bridging oxygen between tetrahedra and a band located in the range 465–475 cm^{-1} attributed to Si–O–Si bending vibration mode. The band located at

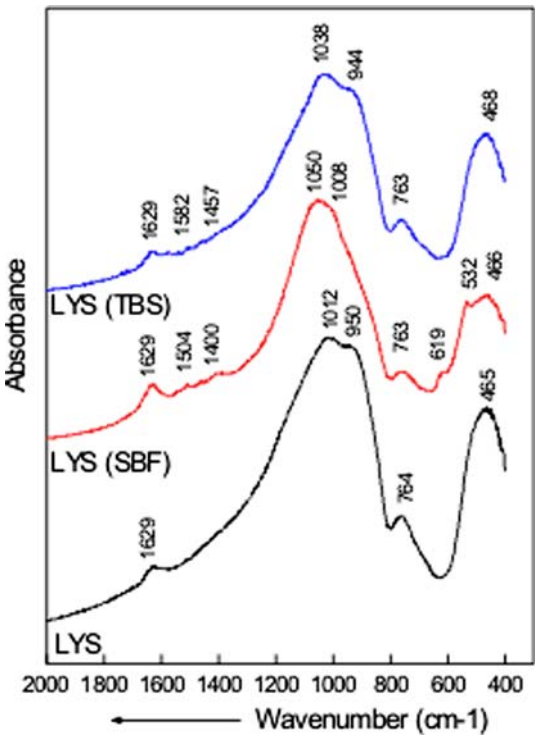

Fig. 12 FT-IR spectra of LYS sample before and after immersion in SBF and TBS

1629 cm^{-1} is assigned to the H–O–H vibration in water molecule [22]. The FT-IR spectra of the as-prepared microspheres are consisted with those reported in the literature for high alkali and alkaline-earth silicate glasses [20].

The FT-IR spectra of the microspheres after immersion in SBF exhibit in addition to the Si–O–Si vibration bands, bands corresponding to the P–O vibration associated with the calcium phosphate layer.

The spectrum of the reference bioactive glass immersed in SBF shows two bands located at 603 cm^{-1} and 564 cm^{-1} attributed to P–O bending vibration in the crystalline hydroxyapatite phase [20, 22]. The band at 1028 cm^{-1} in the unreacted glass spectra, became sharper and is shifted to 1060 cm^{-1}. The shift of this band could be explained by the contribution of the P–O stretching vibration due to the calcium phosphate layer developed on the microspheres surface [19, 24, 25]. Moreover, a band located at 957 cm^{-1} appears in the spectrum, which could be assigned both to the Si–O–2NBO stretching vibration and P–O symmetric vibration of the PO_4^{3-} groups [22, 26].

The decrease in intensity of the band corresponding to the Si–O–2NBO vibration is explained by the high release of the network modifier ions into the solution and silica dissolution, which results in the formation of the Si–OH groups. The condensation and polymerization of these groups leads to the decrease of the non-bridging oxygen number and increase of bridging oxygen number. This fact is clearly indicated by the appearance of the 803 cm^{-1} band in the spectrum, which could be assigned to the Si–O–Si vibration between two adjacent tetrahedra showing the silica-rich layer formation [9, 21]. In addition, the spectrum exhibits a band located at 875 cm^{-1} and a large band in the range 1400–1493 cm^{-1}, assigned to the carbonate vibration mode, which show the incorporation of carbonate anions in the apatite crystal lattice from the SBF solution [19, 21].

The FT-IR spectra of the yttrium bioactive glasses immersed in SBF are shown in Figs. 11 and 12. As can be observed, the twin P–O bend peaks characteristic to the crystalline hydroxyapatite phase is not present in the spectra. Instead a single peak at 538 cm^{-1} and a small shoulder at 617 cm^{-1} corresponding to the P–O bending vibration in calcium phosphate phase is observed [27]. The Y–O vibration modes located at 563 cm^{-1} [28] could also contribute to the intensity of the 538 cm^{-1} peak, but the band is not clearly distinguishable. The band at 1012 cm^{-1} of the unreacted yttrium glasses spectra, became sharper and is shifted to high wave number, at 1056 for the HY1.1 sample and 1050 cm^{-1} for the LYS sample. This band could be assigned both to the Si–O–Si asymmetric stretching vibration mode and P–O stretching vibration. The P–O stretching vibration is superimposed on the bands relative to the Si–O–Si stretching mode and is not clearly distinguishable. The intensity of the bands corresponding to the Si–O–Si symmetric stretching vibration located at 755–764 cm^{-1} decreases after immersion. The Si–O–2NBO vibration band located in the range 934–950 cm^{-1} is shifted to higher wave number after immersion in SBF. The 800 cm^{-1} band corresponding to silica-rich layer formation could not be clearly distinguished in the spectra of yttrium bioactive glasses. The shoulder appeared at 864 cm^{-1} for the HY1.1 and the large band located in the range 1400–1509 cm^{-1} could be assigned to the C–O vibration in the CO_3^{2-} groups [19, 21].

The structural changes occurred in the glass network, caused by soaking in TBS, are shown in the FT-IR spectra of the reacted microspheres. The intensity of the all bands presented in the spectra of the microspheres considerably decreases after immersion period, especially for the HB1 and HY1.1 sample. This fact is attributed to leaching of the glass in the solution. As can be observed from the spectra, the intensity of the Si–O–Si stretching vibration and Si–O–2NBO (Q^2 units) vibration decreased after immersion due to the release of silica and network modifying ions from the microspheres into the solution.

For the bioactive glass microspheres, in addition to the effect of reducing the intensity of the absorption bands, a new band appeared in the spectrum, at 790 cm^{-1}, corresponding to the silica-rich layer formation [9, 21].

For the yttrium glasses, the structural changes can be observed only by reducing the intensity of the Si–O–Si vibration bands. For LYS sample the intensity of the Si–O–Si vibration bands are slightly reduced after immersion, due to the higher stability of the glass network. In case of yttrium bioactive glasses leaching of the glass surface is slower than that of bioactive glass. The silica-rich layer formation on the surface of yttrium bioactive glasses is not clearly indicated by FT-IR or BEI-SEM analysis. However, the linescan EDX analysis on cross section of the reacted yttrium bioactive glass microspheres indicates the presence of a very thin layer rich in silica on their surface after immersion in both used solutions. Moreover, ^{29}Si MAS-NMR results on the yttrium bioactive glass samples after immersion in the SBF solution, indicate the conversion of some Q^2 species into Q^3 species due to the reactions occurred at the glass-solution interface and the presence of a small amount of Q^4 species in the glass structure, corresponding to the formation of a thin silica-rich layer on their surface [29].

Conclusions

FT-IR and BEI-SEM/EDXA results indicate the formation of a silica-rich layer and a crystalline hydroxyapatite phase on the bioactive glass surface in SBF, while on the yttrium bioactive glasses a calcium phosphate phase rich in yttrium was developed. The formation of the silica-rich layer on the yttrium bioactive glass surface is not clearly evidenced by the used investigation methods as it is in the case of reference bioactive glass. However, the linescan EDX analysis indicates the presence of a thin silica-rich layer on the surface of the yttrium bioactive microspheres after immersion in both used solutions. The formation of these reaction layers implies both the release of cations from the glass into the solution and the deposition of different ions from the SBF onto the glass surface.

The analysis of the silica release behaviour in the two used solutions indicates that the addition of yttrium to the bioactive glass composition does not suppress the ion exchange and silica dissolution reactions. ICP-MS results show that the concentration of yttrium released in both solutions is lower than 0.1% of the initial amount of yttrium entering the glass, during the soaking time, supporting the idea of using these glasses for radiotherapeutic purposes.

Acknowledgements Marie Curie Fellowships Program (HPMT-CT-2001-00297) at Åbo Akademi University, Process Chemistry Centre and CNCSIS program (Grant TD 2/32) at Babes-Bolyai University, Faculty of Physics, are acknowledged for the financial support of this work.

References

1. D. E. DAY and T. E. DAY, *in ''Introduction to Bioceramics''*, vol.1 (World Scientific, Singapore, 1993) p. 305
2. J. F. W. NIJSEN, A. D. van het SCHIP, W. E. HENNINK, D. W. ROOK, P. P. van RIJK and J. M. H. de KLERK, *Curr. Med. Chem.* **1** (2002) 73
3. M. KAWASHITA, T. KOKUBO and M. HIRAOKA, in *Proceedings of the 6th International Conference ''Materials in Clinical Applications''*, edited by P. VINCENZINI and R. BARBUCCI (Florence, July 2002), p. 14
4. W. S. ROBERTO, M. M. PEREIRA and T. P. R. CAMPOS, *Artif. Organs* **27**(5) (2003) 420
5. W. S. ROBERTO, M. M. PEREIRA and T. P. R. CAMPOS, *Key Eng. Mater.* **240–242** (2003) 579
6. L. L. HENCH and J. K. WEST, *Life Chem. Rep.* **13** (1996) 187
7. J. P. BORRAJO, J. SERRA, P. GONZALEZ, S. CHIUSSI, B. LEON, M. PEREZ-AMOR, H. YLÄNEN and M. HUPA, *Key Eng. Mater.* **254–256** (2004) 23
8. H. YLÄNEN, K. KARLSSON, A. ITÄLA and H. T. ARO, *J. Non Cryst. Solids* **275**(1–2) (2000) 107
9. L. L. HENCH, *in ''Introduction to Bioceramics''* (World Scientific, Singapore, 1993) p. 319
10. J. E. WHITE and D. E. DAY, *Key Eng. Mater.* **94–95** (1994) 181
11. O. G. KOCH and G. A. KOCH-DEDIC, *Handbuch der Spurenanalyse* (Springer, Berlin 1974) p. 1105
12. D. C. GREESPAN, J. P. ZHONG and G. P. La TORRE, in *Proceedings of the 7th International Symposium on Ceramics in Medicine*, edited by Ö. H ANDERSSON and A. YLI-URPO (Oxford, 1994) p. 28
13. O. ANDERSSON, *The Bioactivity of Silicate Glass*, PhD Thesis, Åbo Akademi University (1990)
14. D. CACAINA, H. YLÄNEN, M. HUPA and S. SIMON, *J. Mater. Sci. Mater. Med.* **17**(8) (2006) 709
15. D. R. LIDE, *The Handbook of Chemistry and Physics*, 78th edn. (1997–1998)
16. P. MCMILLAN, *Am. Mineral.* **69** (1984) 622
17. F. BRANDA, F. A. VARLESE, A. CONSTANTINI and G. LUCIANI, *J. Non Cryst. Solids* **246** (1999) 27
18. J. SERRA, P. GONZALEZ, S. LISTE, S. CHIUSSI, B. LEON, M. PEREZ-AMOR, H. YLÄNEN and M. HUPA, *J. Mater. Sci. Mater. Med.* **13** (2002) 1221
19. J. JONES, P. SEPULVEDA and L. L. HENCH, *J. Biomed. Mater. Res. (App. Biomater.)* **58** (2001) 720
20. J. SERRA, P. GONZALEZ, S. LISTE, C. SERRA, S. CHIUSSI, B. LEON, M. PEREZ-AMOR, H. YLÄNEN and M. HUPA, *J. Non Cryst. Solids* **332** (2003) 20
21. O. PEITL, E. D. ZANATTO and L. L. HENCH, *J. Non-Cryst. Solids* **292** (2001) 115
22. H. A. ELBATAL, M. A AZOOZ, E. M. A. KHALIL, A. S. MONEM and Y. M. HAMDY, *Mater. Chem. Phys.* **80** (2003) 599
23. H. YAN, K. ZHANG, C. F. BLANFORD, L. F. FRANCIS and A. STEIN, *Chem. Mater.* **13** (2001) 1374
24. A. MARTINEZ, I. IZQUIERDO-BARBA and M. VALLET-REGI, *Chem. Mater.* **12** (2000) 3080
25. A. RAMILA and M. VALLET-REGI, *Biomaterials* **22** (2001) 2301
26. Y. M. MOUSTAFA and K. El-EGILI, *J. Non Cryst. Solids* **240** (1998) 144
27. A. CONSTANTINI, R. FRESA, A. BURI and F. BRANDA, *Biomaterials* **18** (1997) 453
28. L. YONGXIU, L. XIAOYUN, W. YIZHENG, L. JUNMING and S. WEILI, *J. Rare Earths* **24** (2006) 34
29. D. CACAINA, M. VASILESCU, H. YLÄNEN, M. HUPA and S. SIMON, *J. Phys. Chem. Solids* (submitted)